Ternary phases (Heusler) in the system Ti–Co–Sn

Andrey Kosinskiy, Department of Physics, University of Oslo, P.O. Box 1048 Blindern, Oslo, Norway
e-mail: andrey.kosinskiy@fys.uio.no
Ole Bjørn Karlsen, Department of Physics, University of Oslo, P.O. Box 1048 Blindern, Oslo, Norway
Magnus H. Sørby, Physics Department, Institute for Energy Technology, P.O. Box 40, Kjeller, Norway
Øystein Prytz, Department of Physics, University of Oslo, P.O. Box 1048 Blindern, Oslo, Norway
Corresponding author, e-mail: oystein.prytz@fys.uio.no

Abstract

Some of the Heusler-phases (XY_2Z and XYZ) are known to have large homogeneity ranges which can be useful for tuning material properties. In this work we have revised the isothermal section of the Ti–Co–Sn system at 973 K (700 °C). 29 ternary compositions, mostly in the regions $TiCo_{2-x}Sn$ for $0 \leq x \leq 1$ and $Ti_{1+y}Co_2Sn_{1-y}$ for $0 \leq y \leq 1$, were prepared by arc-melting, then ball milled and annealed. The resulting annealed powder samples were studied by applying the Rietveld method to X-ray and neutron powder diffraction data. Half-Heusler TiCoSn was not observed. The Heusler phase observed in $TiCo_{2-x}Sn$ has compositions ranging from $TiCo_{1.52}Sn$ to $TiCo_2Sn$ and has the half-Heusler structure where the excess of Co is located on the semi-filled tetrahedral site 4*d* (¾, ¾, ¾) in the space group *F*-43*m*. At 1273 K (1000 °C) this solid solubility is expanded from $TiCo_2Sn$ to TiCo with full solid solubility where Ti is gradually replacing Sn ($Ti_{1+y}Co_2Sn_{1-y}$ for $0 \leq y \leq 1$), while at 973 K (700 °C) there's a small solubility gap for $0.0 \leq y \leq 0.2$.

1 Introduction

Heusler-phases have lately received much attention in the literature, both in fundamental research and in application-focused research areas like thermoelectrics and spin-tronics [1].

Heusler compounds are divided into full-Heusler (fH) and half-Heusler (hH). Both structures are cubic where fH is described with space group *Fm*-3*m* (no. 225, $MnCu_2Al$-prototype), often referred to as XY_2Z, and hH is described with space group *F*-43*m* (no. 216, MgAgAs-prototype), often referred to as *XYZ*, where *X* and *Y* are typically transition metals and *Z* is a main group element.

Early works on the Ti–Co–Sn system indicate the existence of both the fH $TiCo_2Sn$ and the hH TiCoSn [2,3]. These works report a solid solution $TiCo_{2-x}Sn$ that follows Vegard's law only for $x > 0.4$, while below 0.4 the lattice constant of the Heusler-phase stays very close to 6.00 Å. Later studies using Extended X-ray Absorption Fine Structure (EXAFS) and neutron diffraction show that samples with composition TiCoSn after annealing at 1073 K (800 °C) are multi-phase where the Heusler-phase has the composition $TiCo_{1.5}Sn$ and a unit cell close to 6.00 Å [4,5]. However, the most recent studies on the Ti–Co–Sn system again report existence of hH TiCoSn with full solid solubility between hH and fH [6] or a partial solubility [7].

This experimental work deals with annealed powder samples of ternary alloys containing Heusler-phases with elements Ti, Co and Sn. Samples were analyzed mainly by X-ray (XRD) and neutron powder diffraction (ND). The Rietveld method was used to analyze the diffraction data with respect to the compositions and unit cell parameters for the phases as well as the relative phase fractions. Based on these techniques a revised isothermal section at 973 K (700 °C) with the focus on the Heusler-region of the phase diagram Ti–Co–Sn is proposed.

2 Experimental methods

The investigated samples were made by arc melting of elements with purity 99.9 wt. % or better. Arc melting was done in Ti-gettered argon atmosphere in a water-cooled copper hearth and a tungsten electrode. The samples were turned and re-melted 3 times to improve homogeneity. Resulting buttons of about 5 grams were ball milled in argon atmosphere for 6 minutes in SPEX SamplePrep 8000D Mixer/Mill in chromium steel vials (SPEX 8001) with 10 chromium steel balls (14% Cr) of 4 grams each. Sample loss in this whole synthesis process was below 1 % of the initial weight. No contamination of the samples with iron or chromium was detected with EDS in SEM.

The powder samples were annealed in evacuated silica ampoules at the temperatures 973 K (700 °C) and 1273 K (1000 °C) followed by quenching in water. Samples #16-19 (Table 1) were annealed for 21 days at 973 K (700 °C) while the rest of the samples were annealed for 7 days. Annealing at 1273 K (1000 °C) was done for 48 hours and if no severe sample loss (described in the next paragraph) was observed they were annealed for another 48 hours.

We chose to focus on the annealing temperature of 973 K (700 °C) since annealing at both lower and higher temperatures for some of these compositions is problematic. At temperatures 873 K (600 °C) and lower most of the powder samples are not homogenized after annealing for one month. When annealed at temperatures above 1073 K (800 °C), samples that contain the phase Ti_6Sn_5 are found to form an oxide layer on the walls of the silica glass ampoule. The area of the ampoule wall that is in direct contact with the sample becomes coated with a Ti–Sn-oxide, while the rest of the ampoule becomes fully coated with an amorphous Ti-oxide of about 1 μm in thickness. Carbon coating of the ampoule wall does not hinder this process, but it can be suppressed by reducing the inner area of the ampoule, i.e. by soldering a silica rod just above the sample inside the ampoule. The amount of these oxides is relatively low compared to the amount of sample (<1 wt.%), but it involves only two of the components in the sample.

Powder X-ray diffraction (XRD) was done with a Bruker AXS D8 Discover in Bragg-Brentano geometry with Ge(111)-monochromated Cu $K\alpha_1$-radiation and LynxEye™ 1D strip detector with energy filtering to suppress the Co-fluorescence. Data were collected on glass plate holders in the 2θ range of 20°–120° with step size 0.015°. Silicon standard NIST 640d with the lattice constant a = 5.43123 Å was used as internal standard for the XRD measurements. Some samples were also analyzed with neutron powder diffraction (ND) for a different scattering contrast between the elements as compared to X-rays (neutron scattering lengths: b_{Ti} = -3.4, b_{Co}= 2.5, b_{Sn} = 6.2 fm). ND experiments were done at the JEEP II research reactor facility at Kjeller in Norway, on the diffractometer PUS equipped with a focusing composite Ge monochromator and two detector banks with 7 ^{3}He-filled position sensitive detector tubes in each. The sample was contained in a vanadium sample holder with 6 mm inner diameter. Data were collected in the 2θ range 10°–130° with a wavelength of 1.5548 Å for samples $Ti_{33.3}Co_{33.3}Sn_{33.3}$ and $Ti_{28.6}Co_{42.8}Sn_{28.6}$ and 1.5539 Å for the sample

$Ti_{25.0}Co_{50.0}Sn_{25.0}$. Rietveld analysis was carried out with the software Bruker's Topas [8] for XRD and GSAS EXPGUI+ [9,10] for ND. Standard deviations derived from the Rietveld refinements are given in parenthesis after the refined values.

3 Experimental results and discussion

29 different compositions within the Ti–Co–Sn system have been investigated in this work and the samples annealed at 973 K (700 °C) are summarized in Table 1. Space groups of the phases used in Rietveld refinements are listed in Table 2.

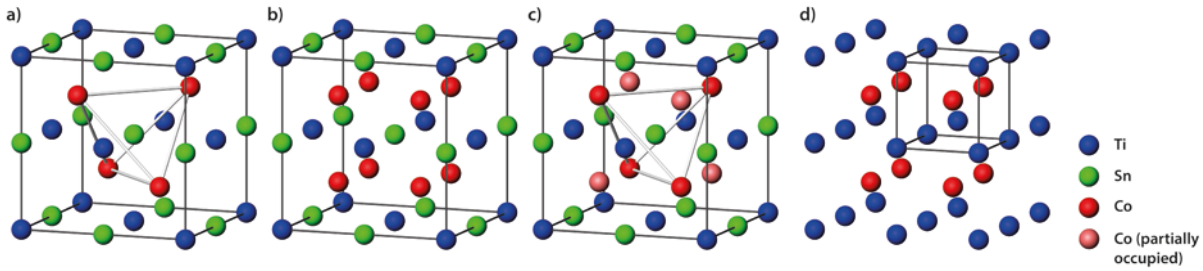

Fig 1: The unit cell of a) half-Heusler (hH) (*F*-43*m*), b) full-Heusler (fH) (*Fm*-3*m*), c) proposed intermediate-Heusler (iH) (*F*-43*m*) and d) TiCo (*Pm*-3*m*). For all of the Heusler structures Ti is in 4*a* (0,0,0); for hH, fH and iH Sn is in 4*b* (½, ½, ½); for hH Co is in 4*c* (¼, ¼, ¼) while 4*d* (¾, ¾, ¾) is unoccupied, while for iH 4*d* (¾, ¾, ¾) is partially occupied; for fH Co is in 8*c* (¼, ¼, ¼). For TiCo Ti is in 1*a* (0,0,0) and Co is in 1*b* (½, ½, ½).

#	Nominal composition Ti-Co-Sn (at. %)	Equilibrated phases	Phase composition (Rietveld)	Relative phase amount (mol. %)	Lattice constant(s) (Å)
1	33.3-33.3-33.3 [a]	$Ti_{1+y}Co_{2-x}Sn_{1-y}$	$TiCo_{1.52(2)}Sn$	70.4(5)	a = 5.9994(2)
		o-Ti_6Sn_5	-	22.1(5)	a = 5.7047(1) b = 91116(1) c = 16.9224(3)
		Liquid (Sn-rich) *	-	7.5(3)	a = 5.8326(3) c = 3.1848(2)
2	30.8-38.4-30.8	$Ti_{1+y}Co_{2-x}Sn_{1-y}$	$TiCo_{1.54(2)}Sn$	90.2(5)	a = 5.9996(2)
		o-Ti_6Sn_5	-	5.8(3)	a = 5.6999(1) b = 9.1056(2) c = 16.898(4)
		Liquid (Sn-rich) *	-	4.0(3)	a = 5.8330(3) c = 3.1852(3)
3	30.3-39.4-30.3	$Ti_{1+y}Co_{2-x}Sn_{1-y}$	$TiCo_{1.54(2)}Sn$	93.5(5)	a = 5.9994(2)
		o-Ti_6Sn_5	-	3.1(3)	a = 5.7127(8) b = 9.115(1) c = 16.952(3)
		Liquid (Sn-rich) *	-	3.4(3)	a = 5.8327(3) c = 3.1842(3)
4	29.9-40.2-29.9	$Ti_{1+y}Co_{2-x}Sn_{1-y}$	$TiCo_{1.55(1)}Sn$	96.9(5)	a = 5.9995(1)
		Liquid (Sn-rich) *	-	3.1(5)	a = 5.8327(4) c = 3.1844(3)
5	29.4-41.2-29.4	$Ti_{1+y}Co_{2-x}Sn_{1-y}$	$TiCo_{1.60(1)}Sn$	96.7(5)	a = 6.0076(1)
		Liquid (Sn-rich) *	-	3.3(5)	a = 5.8329(3) c = 3.1842(3)
6	29.0-42.0.29.0	$Ti_{1+y}Co_{2-x}Sn_{1-y}$	$TiCo_{1.65(1)}Sn$	96.5(5)	a = 6.0181(1)
		Liquid (Sn-rich) *	-	3.5(5)	a = 5.8328(3) c = 3.1842(2)
7	28.6-42.8-28.6 [a]	$Ti_{1+y}Co_{2-x}Sn_{1-y}$	$TiCo_{1.70(1)}Sn$	97.0(5)	a = 6.0268(1)
		Liquid (Sn-rich) *	-	3.0(5)	a = 5.8338(3) c = 3.1846(2)
8	27.4-45.2-27.4	$Ti_{1+y}Co_{2-x}Sn_{1-y}$	$TiCo_{1.88(1)}Sn$	96.9(5)	a = 6.0536(1)
		Liquid (Sn-rich) *	-	3.1(5)	a = 5.8335(7) c = 3.1839(6)
9	26.6-46.7-26.6	$Ti_{1+y}Co_{2-x}Sn_{1-y}$	$TiCo_{1.92(1)}Sn$	97.9(5)	a = 6.0674(1)
		Liquid (Sn-rich) *	-	2.1(5)	a = 5.8334(9) c = 3.1836(7)
10	26.0-48.0-26.0	$Ti_{1+y}Co_{2-x}Sn_{1-y}$	$TiCo_{1.94(1)}Sn$	97.2(4)	a = 6.0712(1)
		CoSn	-	2.8(4)	a = 5.2786(5) c = 4.2701(9)
11	25.6-48.8-25.6	$Ti_{1+y}Co_{2-x}Sn_{1-y}$	$TiCo_{1.98(2)}Sn$	96.7(5)	a = 6.0769(2)
		CoSn	-	3.3(5)	a = 5.2801(4) c = 4.2659(8)
12	25.3-49.4-25.3	$Ti_{1+y}Co_{2-x}Sn_{1-y}$	$TiCo_{2.00(2)}Sn$	97.3(4)	a = 6.0799(3)
		CoSn	-	2.7(4)	a = 5.279(1) c = 4.264(1)
13	25.0-50.0-25.0 [a]	$Ti_{1+y}Co_{2-x}Sn_{1-y}$	$TiCo_{2.00(2)}Sn_{0.97(2)}$	96.4(5)	a = 6.0795(2)
		Co_3Sn_2	-	3.6(5)	a = 4.1126(5)

					c = 5.1864(8)
14	24.4-51.2-24.4	$Ti_{1+y}Co_{2-x}Sn_{1-y}$	$TiCo_{2.00(2)}Sn_{0.96(2)}$	97.4(4)	a = 6.0790(1)
		Co_3Sn_2	-	2.6(4)	a = 4.106(1) c = 5.199(3)
15	23.8-52.4-23.8	$Ti_{1+y}Co_{2-x}Sn_{1-y}$	$TiCo_{2.00(2)}Sn_{0.97(2)}$	96.0(5)	a = 6.0788(1)
		Co_3Sn_2	-	1.7(5)	a = 4.097(2) c = 5.197(4)
		Co	-	2.3(5)	a = 3.5485(9)
16	27.5-50.0-22.5	$Ti_{1+y}Co_{2-x}Sn_{1-y}$	$Ti_{1.05(3)}Co_2Sn_{0.95(3)}$	39.4(4)	a = 6.0820(3)
		$Ti_{1+y}Co_{2-x}Sn_{1-y}$	$Ti_{1.28(3)}Co_2Sn_{0.72(3)}$	59.4(3)	a = 6.0732(4)
		Co_3Ti	-	1.2(2)	a = 3.620(6)
17	30.0-50.0-20.0	$Ti_{1+y}Co_{2-x}Sn_{1-y}$	$Ti_{1.23(1)}Co_2Sn_{0.77(1)}$	97.4(2)	a = 6.0677(5)
		Co_3Ti	-	1.3(2)	a = 3.6202(3)
		c-Co_2Ti / h-Co_2Ti [b]	-	1.3(3)	a = 6.710(3)/ a = 4.747(3) c = 15.52(2)
18	32.5-50.0-17.5	$Ti_{1+y}Co_{2-x}Sn_{1-y}$	$Ti_{1.32(1)}Co_2Sn_{0.68(1)}$	96.9(2)	a = 6.06058(4)
		c-Co_2Ti	-	3.1(2)	a = 6.7116(8)
19	35.0-50.0-15.0	$Ti_{1+y}Co_{2-x}Sn_{1-y}$	$Ti_{1.45(2)}Co_2Sn_{0.55(2)}$	98.8(3)	a = 6.04752(5)
		c-Co_2Ti	-	1.2(3)	a = 6.721(4)
20	40.0-50.0-10.0	$Ti_{1+y}Co_{2-x}Sn_{1-y}$	$Ti_{1.70(2)}Co_2Sn_{0.30(2)}$	99.4(2)	a = 6.03206(5)
		c-Co_2Ti	-	0.6(2)	a = 6.727(5)
21	70.0-10.0-20.0 [c]	$Ti_{1+y}Co_{2-x}Sn_{1-y}$	$Ti_{1.95(3)}Co_2Sn_{0.05(3)}$	-	a = 5.993(1)
		$CoTi_2$	-	-	a = 11.303 (1)
		Ti_3Sn	-	-	a = 5.9156(3) c = 4.7609(4)
22	45.0-45.0-10.0	$Ti_{1+y}Co_{2-x}Sn_{1-y}$	$Ti_{1.79(3)}Co_2Sn_{0.21(3)}$	89.0(7)	a = 6.02410(6)
		$Ti_5Sn_3Co_{1-x}$	Ti_5Sn_3Co	11.0(7)	a = 8.1122(7) c = 5.5308(8)
23	40.0-52.0-8.0	$Ti_{1+y}Co_{2-x}Sn_{1-y}$	$Ti_{1.75(2)}Co_2Sn_{0.25(2)}$	93.1(8)	a = 6.02488(7)
		c-Co_2Ti	-	6.9(8)	a = 6.7152(5)
24	40.0-40.0-20.0	$Ti_{1+y}Co_{2-x}Sn_{1-y}$	$Ti_{1.36(3)}Co_2Sn_{0.64(3)}$	76.7(3)	a = 6.03812(2)
		$Ti_5Sn_3Co_{1-x}$	Ti_5Sn_3Co	23.2(3)	a = 8.1310(2) c = 5.5424(2)
25	35.0-55.0-10.0	$Ti_{1+y}Co_{2-x}Sn_{1-y}$	$Ti_{1.58(1)}Co_2Sn_{0.42(1)}$	81.2(4)	a = 6.02794(5)
		c-Co_2Ti	-	18.8(4)	a = 6.7146(2)
26	30.0-60.0-10.0	$Ti_{1+y}Co_{2-x}Sn_{1-y}$	$Ti_{1.27(2)}Co_{1.95(3)}Sn_{0.73(2)}$	53.9(3)	a = 6.0580(1)
		Co_3Ti	-	26.5(2)	a = 3.6205(4)
		h-Co_2Ti	-	19.6(2)	a = 4.747(1) c = 15.486(6)
27	35.0-35.0-30.0	$TiCo_{2-x}Sn$	$TiCo_{1.57(3)}Sn$	72.7(2)	a = 5.99874(3)
		o-Ti_6Sn_5	-	27.3(2)	a = 5.7142(2) b = 9.1206(4) c = 16.9489(7)
28	30.0-45.0-25.0	$Ti_{1+y}Co_{2-x}Sn_{1-y}$	$Ti_{1.16(2)}Co_{1.74(2)}Sn_{0.84(2)}$	100	a = 6.03625(5)
29	25.0-55.0-20.0	$Ti_{1+y}Co_{2-x}Sn_{1-y}$	$Ti_{1.16(2)}Co_2Sn_{0.84(2)}$	87.4(2)	a = 6.07887(5)

		Co_3Ti	-	1.5(2)	a = 3.6126(6)
		Co	-	11.1(2)	a = 3.5570(1)

Table 1: Equilibrium phase assembly in the investigated samples after annealing at 973 K (700 °C). Obtained by Rietveld refinement of XRD data. Numbers in parenthesis show standard deviations derived from the Rietveld refinements.

[*] liquid solidifies mostly as β-Sn during quenching. Relative phase amount and unit cell parameters are given for this phase.

[a] these samples were analyzed both with XRD and ND

[b] difficult to determine which of the two Co_2Ti phases (cubic or hexagonal) that is present

[c] difficult to quantify relative phase amounts by XRD because $Ti_{1.95(3)}Co_2Sn_{0.05(3)}$ is ductile

- compositions are not refined for these phases

Compound	Space group	Compound	Space group
$Ti_{1+y}Co_{2-x}Sn_{1-y}$	*F*-43*m*	$CoTi_2$	*Fd*-3*m*
$Ti_5Sn_3Co_{1-x}$ [11]	*P*6$_3$/*mcm*	Ti_3Sn	*P*6$_3$/*mmc*
Co	*Fm*-3*m*	o-Ti_6Sn_5	*Immm*
Co_3Ti	*Pm*-3*m*	β-Sn	*I*4$_1$/*amd*
c-Co_2Ti	*Fd*-3*m*	CoSn	P6/*mmm*
h-Co_2Ti	*P*6$_3$/*mmc*	Co_3Sn_2	*P*6$_3$/*mmc*

Table 2: The space group of the observed phases.

We propose a revised isothermal section at 973 K (700 °C) (Fig 2) based on the observed phase relations that are listed in Table 1.

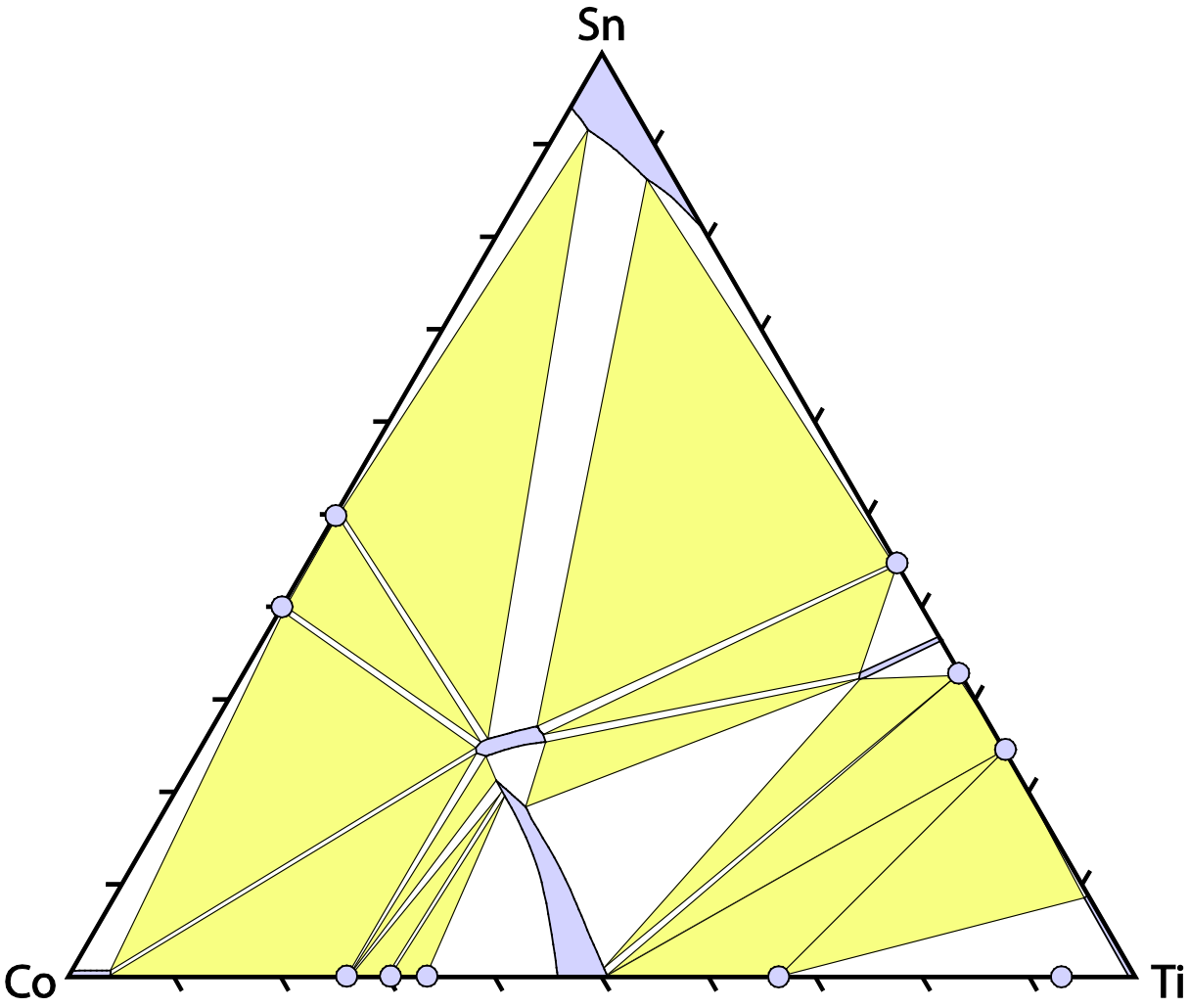

Fig 2: The proposed isothermal section at 973 K (700 °C) of the ternary phase diagram Ti–Co–Sn. The single phase regions are colored in blue and three-phase regions in yellow to facilitate reading. (At 1273 K (1000 °C) the solubility gap between two solubility regions around $Ti_{25}Co_{50}Sn_{25}$ disappears).

A solid solubility range (SSR) $TiCo_{2-x}Sn$ ($x \leq 0.48$) was observed in the investigated temperature interval 973–1273 K (700–1000 °C), however, no hH with composition TiCoSn was found.

The SSR $TiCo_{2-x}Sn$ has space group *F*-43*m* with Wyckoff-positions 4*a* (0,0,0), 4*b* (½, ½, ½) and 4*c* (¼, ¼, ¼), fully occupied with Ti, Sn and Co respectively, while the excess Co is located in the Wyckoff-position 4*d* (¾, ¾, ¾) with site occupancy between 0.52 and 1.0 (Fig 1). A Co 4*d* occupancy of 0.52 gives composition $TiCo_{1.52}Sn$ while occupancy 1.0 gives

composition $TiCo_2Sn$. Rietveld refinement of the diffraction data clearly show that at larger values of *x* (lower amount of Co) the hH structure describes the observed SSR better than fH-structure, but at values of *x* around 0.3 (higher Co-content) these two models become indistinguishable. After all the composition $TiCo_2Sn$ is a fH where the Wyckoff-position 8*c* in the space group *Fm*-3*m* is fully occupied by Co, which is equivalent to having fully occupied Wyckoff-positions 4*c* and 4*d* in the space group *F*-43*m*. For convenience we chose to call this SSR intermediate Heusler (iH) (Fig 1).

Samples with composition $Ti_{33.3}Co_{33.3}Sn_{33.3}$ contain three phases after annealing at 973 K (700 °C). XRD and ND show that the iH-phase is the main phase in these samples and has composition $TiCo_{1.52(2)}Sn$ and a = 5.9994(2) Å (Table 1). After annealing at 1273 K (1000 °C) the sample consist of iH-phase with phase composition $TiCo_{1.60(2)}Sn$ and a = 6.0139(2) Å (70.7 wt%), Ti_6Sn_5 (rt) (4.8 wt%) and Sn-rich liquid that is solidified dominantly into phase the β-Sn (24.5 wt%) during quenching. (On the diffraction pattern of 1273 K (1000 °C) some additional weak reflections are present that can't be indexed to known intermetallic phases of Ti, Co and Sn) These iH-phase compositions make one of the end points of the SSR $TiCo_{2-x}Sn$ and from these observations we can see that the temperature dependence of *x* goes as follows: $x \leq 0.48$ for 973 K (700 °C) and $x \leq 0.40$ for 1273 K (1000 °C).

Anti-site disorder between Co and Ti in the $Ti_{25.0}Co_{50.0}Sn_{25.0}$ (fH composition) has previously been studied by ^{119}Sn Mössbauer spectroscopy and ^{59}Co nuclear magnetic resonance spectroscopy [12]. The reported distortion of a local probe of a sample annealed at 800 K (527°C) for 14 days is $(Ti_{0.91}Co_{0.09})(Co_{1.91}Ti_{0.09})Sn$ with a = 6.0718(3) Å (from XRD). Our observations from XRD show similar lattice constant a = 6.0707(1) Å in a sample with nominal composition $Ti_{25.0}Co_{50.0}Sn_{25.0}$ annealed at 773 K (500 °C), but no anti-site disorder between Co and Ti is observed. Instead the Rietveld refinement shows that the site of Sn (4*b*) is missing 5% scattering intensity in XRD, which might indicate vacancies or a small substitution of the lighter elements Co or Ti on the Sn-site. Samples annealed at 973 K (700 °C) have a larger lattice constant a = 6.0797(1) Å and show no indication of disorder. These values are supported by ND experiments. However samples annealed at 1273 K (1000 °C) have a lower lattice constant a = 6.0721(2) Å for the iH-phase and show no indication of any large disorder in the structure (Table 3).

Annealing temperature	*a* (Å)	Occupation of the element on its Wyckoff position		
		4*a* (Ti)	4*b* (Sn)	4*c* + 4*d* (Co)
773 K (500 °C)	6.0707(2)	1.00	0.95(2)	1.97(2)
973 K (700 °C)	6.0795(2)	1.00	0.97(2)	2.00(2)
1273 K (1000 °C)	6.0721(2)	1.00	1.00(2)	2.00(2)

Table 3: Refinement results from XRD of the iH-phase in samples with composition $Ti_{25.0}Co_{50.0}Sn_{25.0}$ after different annealing temperatures. Position 4*a* is locked to full occupation by Ti in the refinement as normalizing parameter.

It should be emphasized that the samples in the compositional range between $Ti_{33.3}Co_{33.3}Sn_{33.3}$ and $Ti_{25.0}Co_{50.0}Sn_{25.0}$ are not single phase. They consist of the iH-phase together with secondary phases (Table 1). From the relative amounts of phases obtained by Rietveld refinements, without taking any substitutions mechanisms into account, the composition of the iH can be calculated. This shows that composition of the iH is enriched in Ti and Co. This effect is largest for Ti and gives 0.7 at.% excess Ti in the iH for sample $Ti_{25.0}Co_{50.0}Sn_{25.0}$ and 3 at.% for $Ti_{33.3}Co_{33.3}Sn_{33.3}$. One explanation for this could be that the excess of the Ti atoms is allocated on the semi-filled 4*d* site (¾, ¾, ¾), something that will be hard to establish by Rietveld refinement of XRD data since the scattering difference of Co and Ti is so small that XRD is unreliable. For the compositions close to fH the 4*d* site fills up and in sample $Ti_{25.0}Co_{50.0}Sn_{25.0}$ there's no room for allowing Ti in 4*d* (¾, ¾, ¾). From the refinement we see that sites 4*a*, 4*c* and 4*d* are fully occupied with respectively Ti and Co at 973 K (700 °C) (Table 3). However 4*b*, the Sn position, has scattering deficiency of 3%. Vacancies on the Sn site would be in accordance with the observation, but so would also substitution of Ti/Co for Sn be. Later we will show that for $TiCo_2Sn$ substitution of Ti for Sn indeed takes place.

Similar off-stoichiometry has been reported in the closely related system Ti–Ni–Sn. Samples $TiCo_2Sn$ show similar off-stoichiometry where the reported fH has composition $Ti_{23.3}Ni_{52.2}Sn_{24.4}$ after annealing at 950 °C. The authors explained this as Ti/Ni substitution on the Sn-site 4*b* [13]. Off stoichiometry is also reported for the annealed samples TiNiSn containing mostly hH, but phases Ti_6Sn_5 and β-Sn are also present [14].

Samples with compositions $Ti_{33.3}Co_{33.3}Sn_{33.3}$, $Ti_{28.6}Co_{42.8}Sn_{28.6}$ and $Ti_{25.0}Co_{50.0}Sn_{25.0}$, all annealed at 973 K (700 °C) (Table 1, Fig 3), were analyzed with ND. All of these samples give small diffraction peaks at $d = 2.44(1)$ and 1.27(1) Å that fit to a cubic cell with $a = 4.23(1)$ Å, possibly related to a divalent oxide of Ti or/and Co. These peaks were not observed in the XRD patterns. This can possibly be attributed to the specimen size where the amount of analyzed sample for the XRD is in the order of milligrams while the amount of the sample for ND is in the order of grams. In the refinement the peaks were modeled as TiO (*Fm*-3*m*) and were found to make up about 0.5(2) wt.%.

Sample composition	Heusler-phase in the samples			
	973 K (700 °C) annealing		1273 K (1000 °C) annealing	
	a (Å)	Phase composition	*a* (Å)	Phase composition
$Ti_{25.0}Co_{50.0}Sn_{25.0}$	6.0795(2)	$TiCo_2Sn_{0.97(2)}$	6.0721(2)	$Ti_{1.00(1)}Co_{1.99(1)}Sn_{1.00(1)}$
$Ti_{27.5}Co_{50.0}Sn_{22.5}$	6.0820(3) 6.0732(4)	$Ti_{1.05(3)}Co_2Sn_{0.95(3)}$ $Ti_{1.28(3)}Co_2Sn_{0.72(3)}$	6.06780(3)	$Ti_{1.14(2)}Co_{2.00(1)}Sn_{0.86(2)}$
$Ti_{30.0}Co_{50.0}Sn_{20.0}$	6.0677(5)	$Ti_{1.23(1)}Co_2Sn_{0.77(1)}$	6.05992(4)	$Ti_{1.21(2)}Co_{1.95(2)}Sn_{0.79(2)}$
$Ti_{32.5}Co_{50.0}Sn_{17.5}$	6.06058(4)	$Ti_{1.32(1)}Co_2Sn_{0.68(1)}$	6.05117(3)	$Ti_{1.29(2)}Co_{2.00(1)}Sn_{0.71(2)}$
$Ti_{35.0}Co_{50.0}Sn_{15.0}$	6.04752(5)	$Ti_{1.45(2)}Co_2Sn_{0.55(2)}$	6.04323(3)	$Ti_{1.40(1)}Co_{1.96(1)}Sn_{0.60(1)}$

Table 4: Refinement results from XRD of the Heusler-phase in selected samples within composition range $Ti_{1+y}Co_2Sn_{1-y}$ after annealing at 973 K (700 °C) and 1273 K (1000 °C). Values for 973 K (700 °C) are taken from Table 1.

In this work we also have discovered a previously not reported SSR between the compositions $Ti_{25.0}Co_{50.0}Sn_{25.0}$ and $Ti_{50.0}Co_{50.0}$ (Table 4). At 1273 K (1000 °C) there is full solubility of Ti on the Sn-site ($0.0 \leq y \leq 1.0$), but at 973 K (700 °C) there is a solubility gap that reduces the solubility range to $0.2 \leq y \leq 1.0$. Together with the SSR $TiCo_{2-x}Sn$ they form a larger solid solution $Ti_{1+y}Co_{2-x}Sn_{1-y}$ (Fig 1, Fig 4).

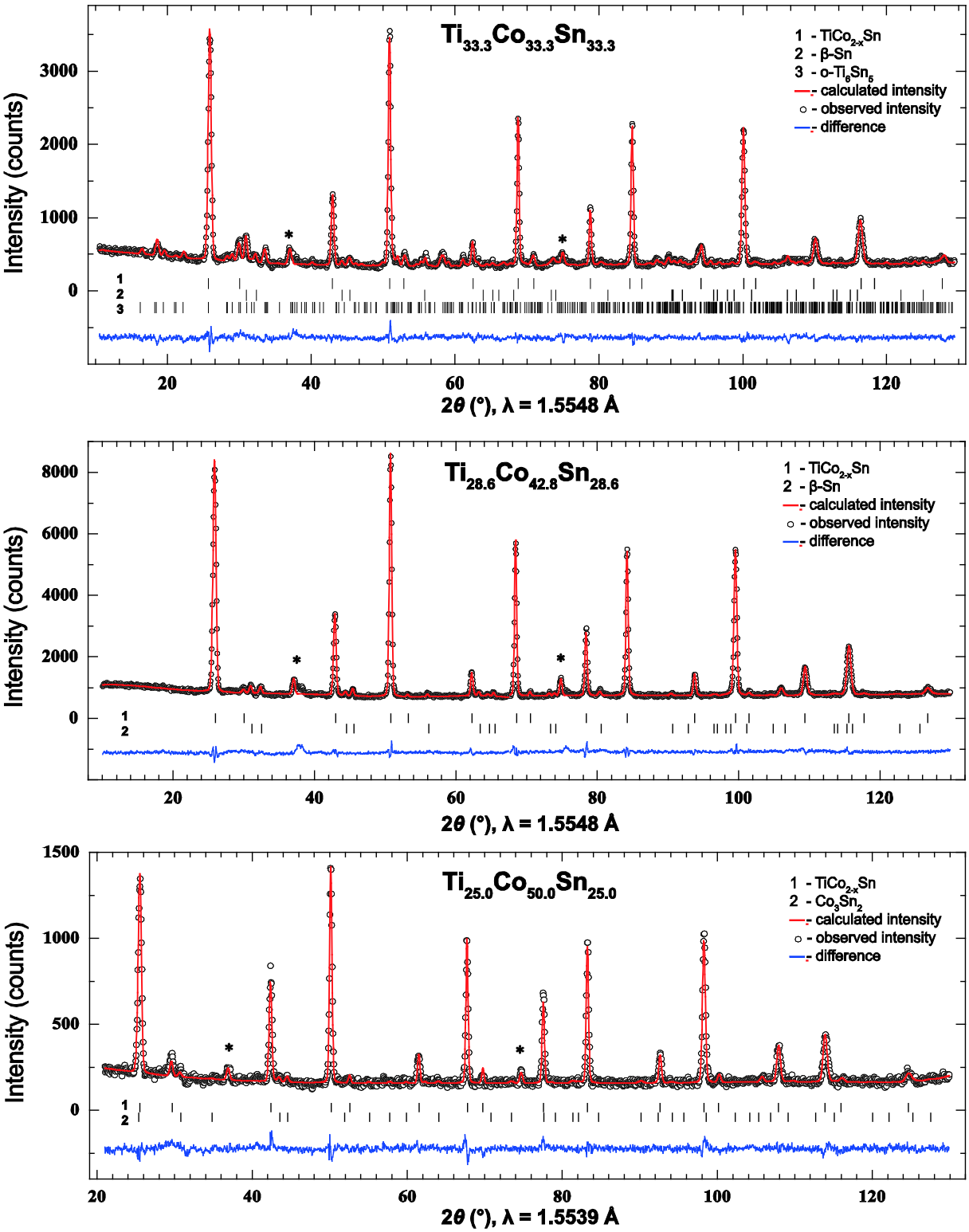

Fig 3: ND data from samples $Ti_{33.3}Co_{33.3}Sn_{33.3}$, $Ti_{28.6}Co_{42.8}Sn_{28.6}$ and $Ti_{25.0}Co_{50.0}Sn_{25.0}$ after annealing at 973 K (700 °C). Peaks marked with (*) were modeled as TiO with a = 4.23(1) Å (see text).

A similarly large solubility region at 1123 K (850 °C) has recently been found in the system Ti–Ni–Sn that extends between TiNi–$TiNi_2Sn$–$TiNi_{1.654}Sn$ [13]. In this system there is a small solubility gap between $Ti_{1.68}Ni_2Sn_{0.32}$ and $Ti_{1.64}Ni_2Sn_{0.34}$.

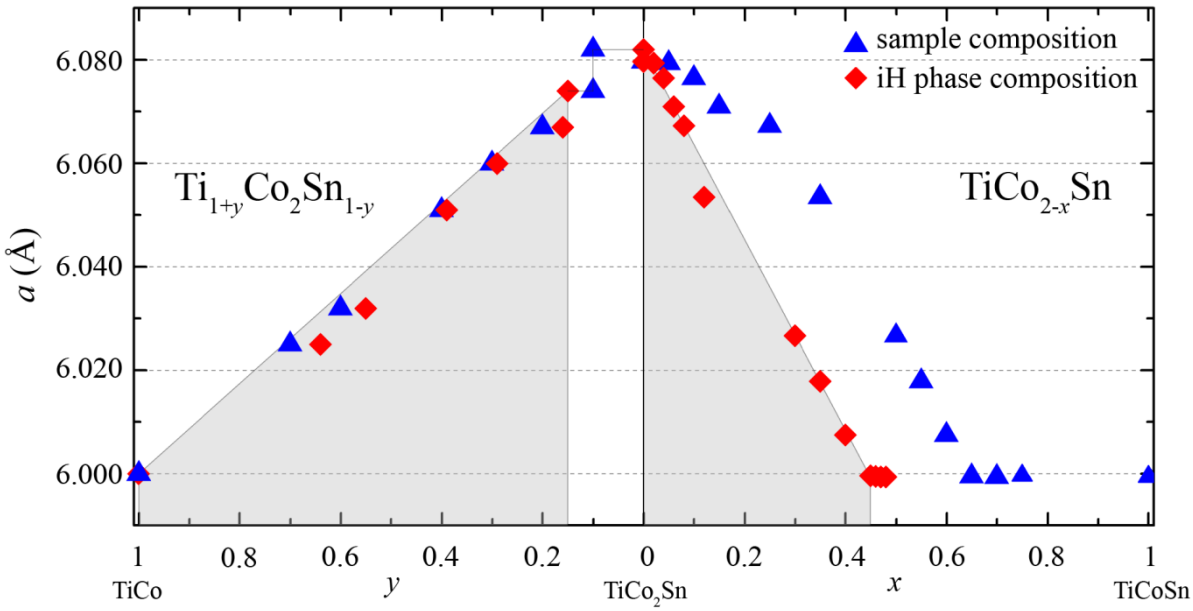

Fig 4: Compositional dependence of the lattice parameters for solid solubility regions $Ti_{1+y}Co_2Sn_{1-y}$ and $TiCo_{2-x}Sn$ in the samples annealed at 973 K (700 °C) (from Table 1). Blue triangles mark the nominal composition of the sample and red diamonds mark the refined iH-phase composition for that sample (sample with $y = 0.1$ contains two iH phases). Homogeneity regions are shaded. The deviation between sample and iH composition is due to the presence of other phases, see text. The value of a for $y = 1$ is taken from ref [15].

There is full solid solubility ($Ti_{1+y}Co_2Sn_{1-y}$ for $0 \leq y \leq 1.0$) in the samples within this compositional range after annealing at 1273 K (1000 °C). However, samples annealed at 973 K (700 °C) indicate a solubility gap in the composition range $0.0 \leq x \leq 0.2$. This manifests itself as shoulders on the iH-peaks in the XRD data (Fig 5). The shape of this shoulder remains the same even after increased annealing time up to 1 month at 973 K (700 °C). After annealing at 1273 K (1000 °C) the diffraction data of these samples are easily fitted with one Heusler-like phase with sharp peaks. Re-annealing down from 1273 K (1000 °C) makes the peaks broader, which indicates phase separation, and shifts the a-axis back to larger values. Since the shoulder reappears after re-annealing there are grounds to assume that compositions

with $0.0 \leq y \leq 0.2$ experience a transition from a single-phase to a two-phase area somewhere between 973 K (700 °C) and 1273 K (1000 °C). Surprisingly the lattice constants *a* for the iH-phases within this SSR get noticeably lower with the increase in the annealing temperature, for instance $Ti_{35.0}Co_{50.0}Sn_{15.0}$ contains iH-phase with *a* = 6.04752(5) Å after annealing at 973 K (700 °C) and 6.04323(3) Å after annealing at 1273 K (1000 °C) (Table 4, Fig 5).

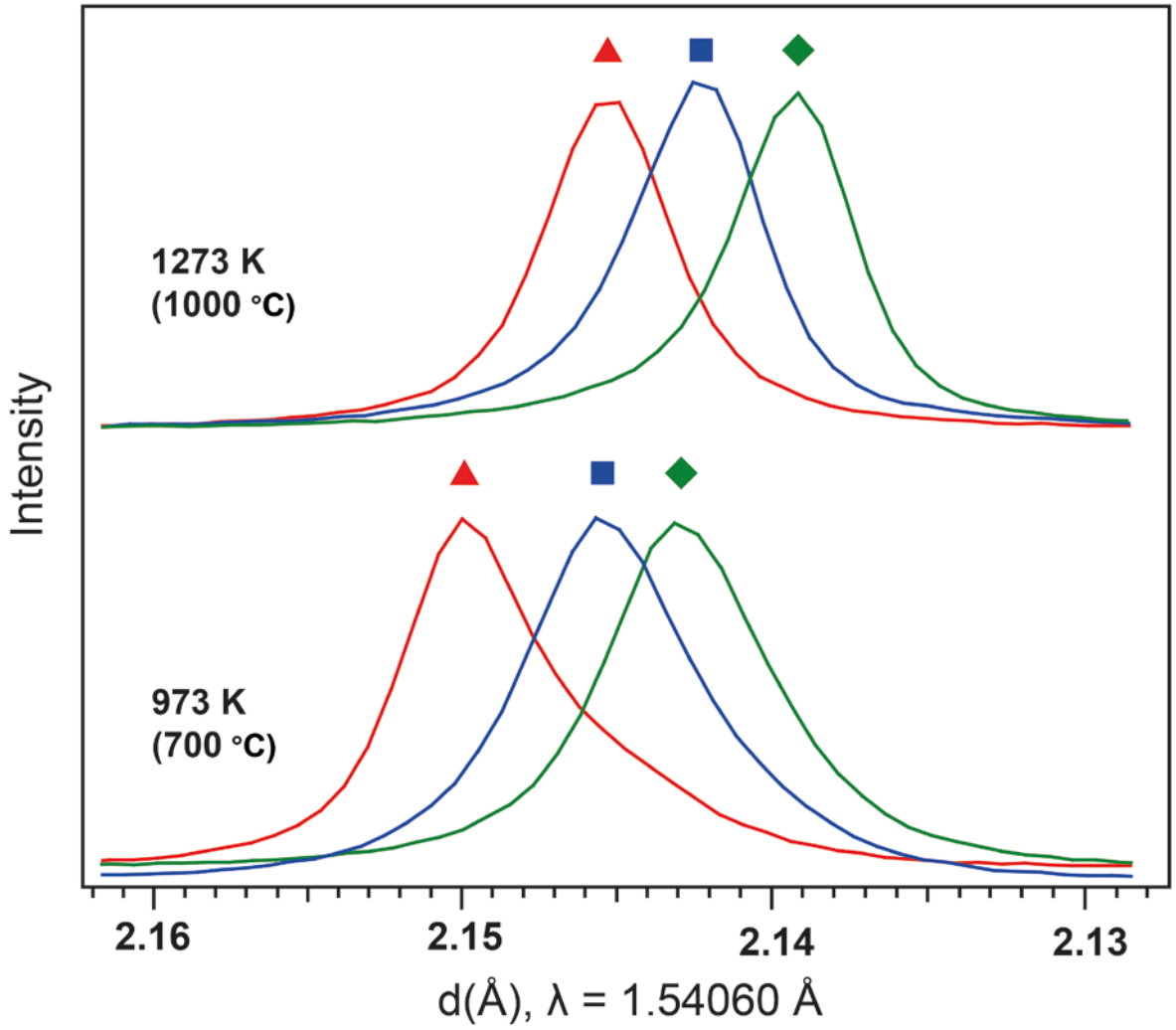

Fig 5: 220-peaks of the iH phases in samples $Ti_{27.5}Co_{50.0}Sn_{22.5}$ (red triangle), $Ti_{30.0}Co_{50.0}Sn_{20.0}$ (blue square) and $Ti_{32.5}Co_{50.0}Sn_{17.5}$ (green diamond) after annealing at 973 K (700 °C) and 1273 K (1000 °C). A distinctive shoulder is visible for the $Ti_{27.5}Co_{50.0}Sn_{22.5}$ annealed at 973 K (700 °C).

These two solid solubility ranges form together a continuous solid solution at 1273 K (1000 °C) that may schematically be written as $Ti_{1+y}Co_{2-x}Sn_{1-y}$ for ($0 \leq x \leq 0.40$ and $y = 0$; or

$0 \leq y \leq 1$ and $x = 0$) while at 973 K (700 °C) there's a gap in the composition and thus the solid solution can be written as ($0 \leq x \leq 0.48$ and $y = 0$; or $0.2 \leq y \leq 1$ and $x = 0$) (Fig 4). This fact that none of the samples on the compositional line $TiCo_2Sn$–TiCoSn are single phase at 973 K (700 °C) complicates the representation of the figure.

4 Conclusions

In this work we have revised the isothermal section at 973 K (700 °C) of the ternary system Ti–Co–Sn. The main focus of the study was to explore the phase relations around the Heusler-phases. The stoichiometric half-Heusler TiCoSn was not found to be present. Solid solution from $TiCo_2Sn$ to $TiCo_{1.52}Sn$ at 973 K (700 °C) has been established. In addition a solid solution between $TiCo_2Sn$ and TiCo, with Ti substitution for Sn, has been shown to exist. This solid solution is full at 1273 K (1000 °C) but has a miscibility gap at 973 K (700 °C). The full solubility range of the Heusler related phases may be written as $0 \leq x \leq 0.48$ and $y = 0$; or $0.2 \leq y \leq 1$ and $x = 0$ at 973 K (700 °C) and $0 \leq x \leq 0.40$ and $y = 0$; or $0 \leq y \leq 1$ and $x = 0$ at 1273 K (1000 °C).

Acknowledgments

This research was partially supported by the research project THELMA (Project No. 228854) funded by The Research Council of Norway. The authors furthermore want to thank the The Basic and Applied ThermoElectric intiative (BATE) and especially professor emeritus Johan Taftø for initiation, inspiration and guidance into the realm of thermoelectricity.

References

[1] T. Graf, C. Felser and S. S. P. Parkin: *Prog. Solid State Ch.*, 2011, 39, p. 1

[2] J. Pierre, R.V. Skolozdra and Yu.V. Stadnyk: *J. Magn. Magn. Mater.*, 1993, 128, p. 93

[3] R.V. Skolozdra, Yu.V. Stadnyk, Yu.K. Gorelenko and E.E. Terletkaya: *Sov. Phys. Solid State*, 1990, 32 , p. 1536

[4] T. Nobata, G. Nakamoto, M. Kurisu, Y. Makihara, T. Tokuyoshi and I. Nakai: *Jpn. J. Appl. Phys.*, 1999, suppl. 38-1, p. 429

[5] T. Nobata, G. Nakamoto, M. Kurisu, Y. Makihara, K. Ohoyama and M. Ohashi: *J. Alloys Compd.*, 2002, 347, p. 86

[6] Yu. Stadnyk, L. Romaka, A. Horyn, A. Tkachuk, Yu. Gorelenko and P. Rogl: *J. Alloys Compd*, 2005, 387, p. 251

[7] C. Colinet, J.-C. Tedenac and S. G. Fries: *CALPHAD*, 2009, 33, p. 250

[8] A. A. Coelho: Bruker AXS. Karlsruhe, Germany, 2006

[9] A. C. Larson and R.B. Von Dreele: Los Alamos National Laboratory Report LAUR, 2000, p. 86

[10] B. H. Toby: *J. Appl. Cryst.*, 2001, 34, p.210

[11] J. C. Schuster , M. Naka and T. Shibayanagi: *J. Alloys Compd.*, 2000, 305, p. L1

[12] H. C. Kandpal, V. Ksenofontov, M.Wojcik, R. Seshadri and C. Felser: *J. Phys. D*, Appl. Phys., 2007, 40, p. 1587

[13] M. Gürth, A. Grytsiv, J. Vrestal, V. V. Romaka, G. Giester, E. Bauer and P. Rogl: *RSC Advances*, 2015, 5, p. 92270

[14] J. E. Douglas, C. S. Birkel, N. Verma, V. M. Miller, M.-S. Miao, G. D. Stucky, T. M. Pollock and R. Seshadri: *J. Appl. Phys.*, 2014, 115, p. 043720

[15] T. Takasugi and O. Izumi: *Phys. status solidi A*, 1987, 102, p. 697